

Seasonality can induce coexistence of multiple bet-hedging strategies in *Dictyostelium discoideum* via storage effect

Ricardo Martinez-Garcia and Corina E. Tarnita

*Department of Ecology and Evolutionary Biology,
Princeton University. Princeton NJ, 08544. USA*

Dictyostelium discoideum has been recently suggested as an example of bet-hedging in microbes. Upon starvation a population of unicellular amoebae splits between aggregators, which form a fruiting body made of a stalk and resistant spores, and non-aggregators, which remain as vegetative cells. Spores are favored by long starvation periods, but vegetative cells can exploit resources in fast-recovering environments. The investment in aggregators versus non-aggregators can therefore be understood as a bet-hedging strategy that evolves in response to stochastic starvation times. A genotype (or strategy) is defined by a different balance between each type of cells. In this framework, if the ecological conditions on a patch are defined in terms of the mean starvation time (i.e. time between onset of starvation and the arrival of a new food pulse), a single genotype dominates each environment, which is inconsistent with the huge genetic diversity observed in nature. Here we investigate whether seasonality, as represented by a periodic alternation in the mean starvation times, allows the coexistence of several strategies in a single patch. We study this question in a non-spatial (well-mixed) setting where different strains compete for a pulse of resources. We find that seasonality, which we model via two seasons, one wet and one dry, induces a temporal storage effect that can promote the stable coexistence of multiple genotypes. Two conditions need to be met. First, the distributions of starvation times in each season cannot overlap in order to create two well differentiated habitats within the year. This excludes all those distributions in which the mode of the distribution (i.e. the most frequent value) is independent of its mean value, such as the exponential. Second, numerous growth-starvation cycles have to occur during each season to allow well-adapted strains to grow and survive the subsequent unfavorable period. These conditions allow the coexistence of two bet-hedging strategies. Additional tradeoffs among life-history traits can expand the range of coexistence and increase the number of coexisting strategies, contributing towards explaining the genetic diversity observed in *D. discoideum*. Although focused on this cellular slime mold, our results are general and may be easily extended to other microbes.

I. INTRODUCTION

In *Dictyostelium discoideum* starvation triggers the aggregation of free-living amoebae and the development of a multicellular fruiting body. During aggregation, cells do not exclude genetic non-relatives and therefore chimeric fruiting bodies (made of at least two genotypes) can be formed. Fitness in *D. discoideum* has been traditionally equated to the number of reproductive spores [1]; in lab experiments, this has led to the establishment of a linear hierarchy of genotypes (or strains) that reflects the overrepresentation of certain genotypes in the spores of chimeras [2]. This result suggests a decrease in the number of existing strains, which is incompatible with the huge diversity observed in natural isolates of *D. discoideum* [3]. Recent studies have suggested however that this inconsistency arises from the one to one correspondence between spore number and fitness, which is likely incomplete since it ignores various other fitness components, such as spore viability [4], and the role of vegetative non-aggregating cells [5, 6]. The existence of several tradeoffs among these components turns fitness into a more complex quantity in *D. discoideum* [4, 7]. However, even in this more comprehensive framework coexistence remains puzzling and additional mechanisms need to be considered.

For the purpose of this study each strain is defined by a certain set of discrete traits and multi-strain coexistence can be studied within the well-established theoretical framework of species coexistence. Classical results from community ecology establish that only one species can survive in communities where different species compete for one common resource [8–10]. Coexistence requires that different species be heterogeneous in the way they respond to and affect their biotic and abiotic environment [11–14]. *D. discoideum* presents, however, an additional issue: the different strains are hypothesized to hedge their bets in response to uncertain environmental conditions. Upon starvation, amoebae diversify their commitment in the formation of the fruiting body. As a result, some of them remain as non-aggregating vegetative cells. According to some models [5, 6] this population partitioning could represent a risk-spreading reproductive strategy. Non-aggregators could readily start reproducing after resources replenishment, but they are less resistant to starvation. On the other hand, spores survive longer starvation times but pay a cost when food recovers fast due to a time-consuming fruiting body development and delayed germination. In this theoretical framework, how much a strain invests in each type of cell (aggregating versus non-aggregating) is a bet-hedging trait that evolves in response to uncertainty in the starvation times: slower-recovering environments, represented by larger mean values of the starvation time, select for more spores; faster-recovering environments, where starvation times are typically shorter, select

for a higher investment in non-aggregators [5, 6].

Spatial heterogeneity as a promoter of coexistence has recently been studied in *D. discoideum* [6] and low-to-moderate dispersal between multiple patches has been theoretically shown to allow the coexistence of several *D. discoideum* strains. Here we explore the role of temporal heterogeneity (in this case seasonality) in fostering coexistence. This turns out to be challenging because bet-hedging strategies are plastic, which allows them to average across different ecological conditions by reducing the variance of the fitness in order to minimize the risks of complete reproductive failure. This plasticity comes at the expense of diminishing the mean fitness, since some offspring are always maladapted to a subset of environmental conditions [15–19]. In the presence of seasonality, which introduces a second characteristic scale in the environment by periodically switching its statistical properties, the optimal bet-hedging strategy may change. Hence, it is hard to discern when seasonality will cause the evolution of a new optimal bet-hedging strategy that averages over both seasons, and when it will lead to the coexistence of two season-specialist bet-hedging strategies (i.e. temporal niche partitioning [20–24]).

Temporal coexistence of bet-hedging species has been studied both theoretically [11, 25] and experimentally [26] in seed banks of annual plants, one of the classic and better studied instances of bet-hedging [27–29]. Periodic changes in the ecological conditions during the year mediate the coexistence of several strains through a temporal storage effect [11, 24, 30] if three general requirements are satisfied: (i) changes in the environmental conditions favor different species (temporal niche partition), (ii) the rate at which populations decline together with the temporal scale of the environmental fluctuations avoids the extinction of non-favored species and (iii) the intensity of the interspecific competition changes with the ecological conditions, so populations can recover from very low sizes [31–33].

Here we aim to: (i) provide a theoretical starting point to unveil the ecological conditions that promote coexistence of microbial bet-hedging strategies in the presence of temporal heterogeneity and tradeoffs between multiple life-history traits and (ii) make testable predictions to stimulate future empirical work. Although we focus on *D. discoideum* in particular, we hypothesize that these results might extend to the study of diversity in microbial populations in general [34–36], where bet-hedging has been frequently reported [37–39].

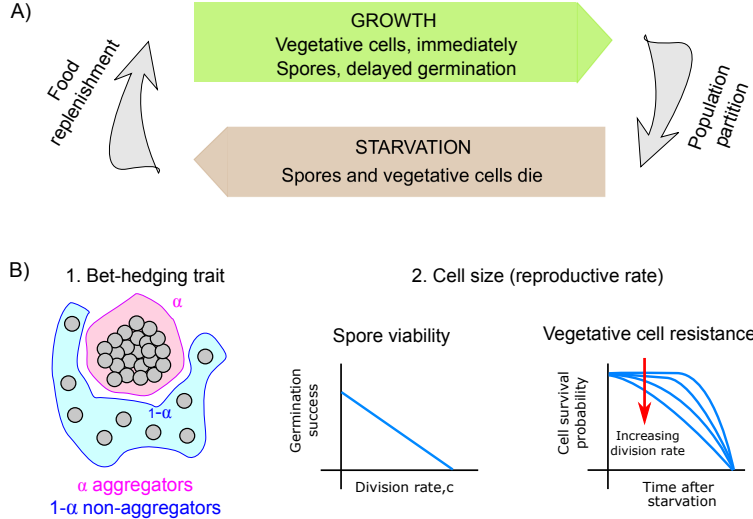


FIG. 1. *D. discoideum* life cycle and fitness tradeoffs. A) The life cycle of *D. discoideum* consists of a series of growth and starvation cycles. The growing phase starts with the arrival of a pulse of resources and aggregation, which in our model is represented by the population partition between spores and series of growth and starvation cycles. The growing phase starts with the arrival of a pulse of resources vegetative cells, occurs after food depletion. B) Three different tradeoffs are considered. The first one, between aggregating and staying vegetative determines the bet-hedging strategy. Two additional tradeoffs yield between spore viability and resistance to starvation and division rate (negatively correlated to the cell size).

II. MODEL

We consider a well-mixed model for the life cycle of *D. discoideum* (Fig. 1A) where different strains compete for a pulsed resource R [6]. The fitness of each strain is given by two traits (investment in spores and division rate) and involves two major tradeoffs that are optimized in order to adapt to different ecological scenarios: (i) spore production versus number of non-aggregating vegetative cells and (ii) reproduction rate versus cell size, which is correlated with resistance to starvation [40] and spore viability [4]. The latter tradeoff relies on our assumption that cell/spore size is inversely correlated with the reproduction rate. A summary of the parameters and traits included in the model as well as their numerical values is provided in Table I.

The two traits of a genotype are: α and c . α is the bet-hedging trait and gives the fraction of cells that aggregate upon starvation. The limits $\alpha = 0$ and $\alpha = 1$ capture the extremes where either all cells remain vegetative, or they all aggregate, respectively; intermediate values represent a continuum of bet-hedging strategies. c is the division rate when resources are abundant. Resources

are consumed by feeding populations that grow according to Monod-like dynamics [41]

$$\dot{x}_{\alpha,c} = \frac{cR}{R + R_{1/2}} x_{\alpha,c}, \quad (1)$$

$$\dot{R} = -\frac{R}{R + R_{1/2}} \sum_{\alpha,c} c x_{\alpha,c}, \quad (2)$$

where $x_{\alpha,c}$ is the population size of each strain and $R_{1/2}$ is the abundance of resources at which the growth rate is half of its maximum c . As single cells only die due to starvation, we neglect the death term during the feeding phase. Once resources are completely consumed we assume that aggregation takes place instantaneously and the population splits into a fraction α of aggregators and a fraction $1 - \alpha$ of non-aggregators (Fig. 1B). Within an aggregate only about 80% of the cells become reproductive spores. The other 20% die in the process of stalk formation. To include this stalk/spores differentiation and obtain the number of reproductive spores we multiply the fraction of aggregated cells by a factor $s = 0.8$. Then, the starvation phase starts and it ends with the arrival of the next pulse of resources after a starvation time, T_{st} , has elapsed. Unlike previous studies that used either exponential [6] or uniform distributions with a fixed width [5], we want to explore scenarios in which the mean value of the starvation times and the intensity of their fluctuations are independent of each other. Thus, we will take the starvation times to be distributed according to truncated normal distributions. The sequence determined by growth-aggregation-starvation is repeated indefinitely (Fig. 1A). For simplicity, we will keep the initial size of the food pulses, R_0 , constant and encapsulate the entire ecological context in the starvation times such that worse environmental conditions are represented by longer starvation times. Therefore, the environmental quality decreases with increasing starvation times.

During the starvation phase there is no reproduction and only cellular death takes place; however, spores and vegetative cells show different behaviors. Dormant spores die at a very small constant rate, while vegetative cells follow a survival curve with a time-dependent death rate. Experimental work on *D. discoideum* has demonstrated that vegetative non-aggregating cells resist the first hours after resources depletion by consuming their own organelles and cytoplasmic resources [42]. Therefore, bigger cells (here assumed to result from lower division rates) are more likely to survive during the first hours of starvation. To reflect these observations, we choose a family of survival curves given by

$$S(t) = \frac{\exp(-(\mu t)^{\beta(c)}) - \exp(-(\mu T_{sur})^{\beta(c)})}{1 - \exp(-(\mu T_{sur})^{\beta(c)})}, \quad (3)$$

where $\beta(c)$ is a linear function of the division rate that accounts for the cost of dividing faster. Therefore, a genotype with division rate c has a specific value $\beta(c)$ that determines its survival

probability at short times. As higher values of β result in survival curves with a lower slope at short times, we choose the functional form $\beta(c)$ such that: (i) $\beta(c) > 1$ for all c , to capture the fact that all the survivorship curves decay slowly during the cell autophagy period (short times after starvation); and (ii) $\beta(c)$ is a decreasing function of the growth rate, to capture the tradeoff between cell size and the resistance to starvation [4]. Strains with a higher reproduction rate produce smaller cells that are less resistant to starvation. Their survivorship curves hence show a faster decay at short times (Fig. 1B) (see Table I for an explicit expression for β). T_{sur} is the maximum lifetime of a vegetative cell and μ is the rate at which the death rate of a cell changes with time. Given these choices for the death of both populations, we can obtain the number of spores and vegetative cells at the end of the starvation period by evaluating the following expressions

$$x_{\alpha,c}^s(t = T_{st}) = x_{\alpha,c}^s(t) e^{-\delta T_{st}}, \quad (4)$$

$$x_{\alpha,c}^v(t = T_{st}) = x_{\alpha,c}^v(t) S(T_{st}). \quad (5)$$

After the starvation phase is over, a new pulse of food arrives. Then, surviving vegetative cells start feeding and reproducing instantaneously according to Eq. (1). Dormant spores however have to follow a complete germination process during which they continue to die at rate δ . Once germination is completed, which takes time τ , only a fraction $\rho(c)$ of the spores are viable and become active cells. As smaller spores are less viable [4], and we assume that cell/spore size is inversely correlated with the reproductive rate, ρ is a decreasing function of the reproduction rate. For simplicity we fix a linear dependency between spore viability, ρ , and reproduction rate c (see Table I for an explicit expression, Fig. 1B).

III. RESULTS AND DISCUSSION

A. One environmental scale: the emergence of bet-hedging

We first investigate how environmental fluctuations (stochasticity in the times between the onset of starvation and the appearance of the next food pulse) drive the emergence of bet-hedging strategies that are defined by intermediate values of α . Previous studies have explored this question using either an exponential [6] or a uniform distribution of fixed width [5]. Here we focus on truncated normal distributions to explore a different scenario, one in which the amplitude of the environmental variability (standard deviation of the distribution of starvation times, σ) is independent of the mean starvation time (Fig. 2D, A). For a better comparison with the case in which the amplitude of the environmental variability and the mean starvation times are coupled, we also

Description	Symbol	Value	Units
Rate of change of the vegetative cell death rate	μ	2×10^{-3}	hour ⁻¹
Maximum lifetime of a vegetative cell	T_{sur}	200	hour
Spore germination time	τ	4	hour
Spore mortality rate	δ	2×10^{-4}	hour ⁻¹
Fraction of aggregators that become spores	s	0.8	—
Initial food pulse	R_0	10^8	# cells
Half-saturation constant of resources consumption	$R_{1/2}$	$0.1R_0$	# cells
<hr/>			
Division rate	c	0.173 / varied	hour ⁻¹
Spore viability	ρ	$1.1 - 2c$	—
Resistance to starvation	β	$3.1 - 4c$	—
Investment in aggregators	α	varied	—

TABLE I. Definition of the parameters and their values. The lower part of the table includes the traits that are allowed to evolve in some of the sections and the implementation of the tradeoffs

explore the outcome of exponentially distributed starvation times. To isolate the effect of temporal disorder on the bet-hedging trait we fix the value of the division rate and the tradeoffs related to it: spore viability and vegetative cell resistance to starvation (Table I). However, in Section III C we analyze the full model.

In the absence of seasonality, the temporal component has a single characteristic scale during the year, which is given by the mean starvation time λ_T . If the environment is deterministic, starvation times are fixed and coincide with this mean value (red squares in Fig. 2A and Fig. 2B; the red line in Fig. 2D shows the distribution of starvation times). In this case, consistent with previous findings [5, 6], only pure strategies are selected for: $\alpha = 1$ (only spores) if $T_{st} > T^*$ and $\alpha = 0$ (only vegetative cells) otherwise. The transition point, $T^* = 170$ hours, is of the order of the maximum lifespan of vegetative cells. In the following we will refer to environments with a mean starvation time below T^* as good environments and to those above this threshold as harsh environments. If the environment is stochastic (i.e. characterized by fluctuations in starvation times), then intermediate investments in spores are selected for, which represent bet-hedging strategies. We introduce these fluctuations by drawing the length of each starvation period from a distribution with mean λ_T . Two classes of distributions are investigated; (i) exponential distributions (Fig. 2A, 2B) and (ii) a family of truncated normal distributions with different amplitudes (Fig. 2C, 2D; A). The truncation of the distribution, with a cutoff at $T_{st} = 0$, avoids unrealistic negative values for the starvation times. In addition, due to this cutoff, the mode of the distribution (i.e, the most frequent value

for the starvation times) decreases when the standard deviation increases and the mean value is kept constant. Consistently with [5, 6], we find that higher investments in spores are favored as the environments become harsher (i.e. are characterized by larger mean starvation times) (Fig. 2A and 2C). For the truncated normal distribution, increasing the amplitude of the variation in the starvation times promotes the evolution of bet-hedging both in good and in harsh environments. In harsh environments, however, bet-hedging requires higher amplitudes. Strategies with a higher investment in nonaggregators are riskier and more strongly affected by long starvation times than those with a higher investment in spores are affected by short starvation periods. Due to the truncation at $T_{st} = 0$, the mode of the distribution approaches zero as its variance increases. This makes short starvation periods more frequent, which penalizes a pure strategy with $\alpha = 1$. In fact, the exponential distribution can be seen as a limit case of a truncated normal distribution with a very high standard deviation (see orange line in Fig. 2D and the distribution in Fig. 2B), which explains the higher impact of exponential variability on the winning strategy in harsh environments (black squares in Fig. 2A).

B. Two environmental scales: the effect of seasonality on strain coexistence

Next we introduce seasonality in the model, so the environmental heterogeneity has two different temporal scales: (i) the mean starvation time within each season and (ii) the length of each season, which gives the transition rate between mean starvation times. We consider the simplest scenario: a combination of a wet and a dry season. Due to the stochasticity in the starvation times, the length of each season cannot be controlled, so we introduce two parameters, T_{wet} and T_{dry} , that provide a lower bound to the length of the seasons rather than their exact duration. In the implementation of the model, sequences of growth-starvation cycles occur within a season until its length is exceeded. The horizontal bars in Fig. 3 provide an example of this. The seasons usually exceed T_{dry} and T_{wet} and the switch takes place at the end of the first starvation period after these values have been surpassed. This indicates the end of the season and the beginning of the next one. In the following, however, we will refer to T_{wet} and T_{dry} as the length of each of the seasons for simplicity. We study the outcome of two possible scenarios: (i) a severe dry season that consists of a very large starvation period without nutrient replenishment (Fig. 3A) and (ii) a milder dry season during which resources do replenish but are followed by starvation times that are, on average, larger than those of the wet season ($\lambda_{dry} > \lambda_{wet}$) (Fig. 3B).

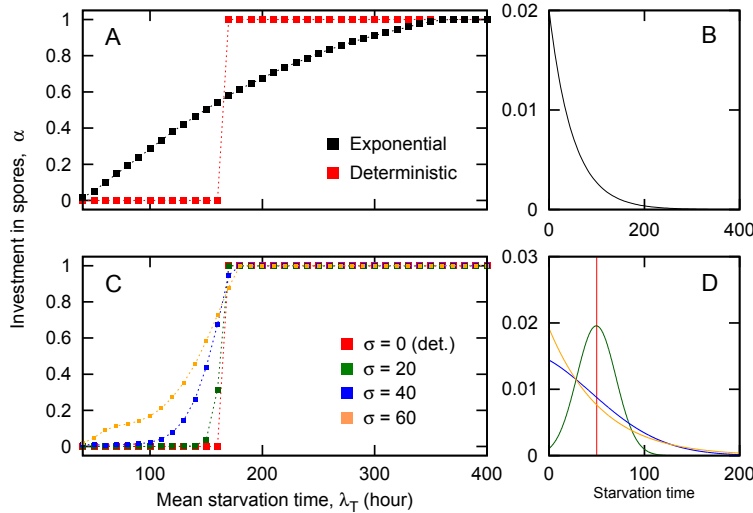


FIG. 2. Winning genotype in deterministic and stochastic environments and distributions of starvation times. The squares in panels A and C represent the optimal investment in spores and the dashed lines are interpolations. Simulations are started with 1001 genotypes uniformly distributed between $\alpha = 0$ and $\alpha = 1$ and the winners obtained as the most abundant strains after 2×10^8 hours. A single run is used in the deterministic cases and averages over 20 realizations in stochastic environments. A) Red squares correspond to the deterministic case and black squares to exponentially distributed starvation times. B) Exponential distribution for the starvation times with mean value $\lambda_T = 50$ hour. C) From top to bottom (increasing square size): $\sigma = 60$ (orange), $\sigma = 40$ (blue), $\sigma = 20$ (green), $\sigma = 0$ deterministic (red). D) Truncated normal distributions for the starvation times with mean value $\lambda_T = 50$ hour and increasing σ (same color code as in panel C). The red line represents a Dirac delta distribution.

1. Severe dry season: no resource replenishment

We first investigate the scenario in which resources do not come back to the system during the dry season; in this case, the length of the season is equal to the length of the sole starvation time. The wet season however consists of several growth/starvation cycles with starvation times sorted either from a truncated normal distribution of mean value λ_{wet} and standard deviation σ or from an exponential distribution of mean value λ_{wet} . We will focus on the effect of dry season length and wet season starvation times; therefore, the parameters of interest are T_{dry} and λ_{wet} (and σ for truncated normal distributions), while $\lambda_{dry} = T_{dry}$ and $T_{wet} = 1$ year - T_{dry} are determined by the length of the dry season. As before, these quantities provide a lower limit for the length of the seasons (T_{dry} and T_{wet}). The distribution of starvation times over many years (Fig. 3A) has two components: (i) a Dirac delta distribution centered at $\lambda_{dry} = T_{dry}$ for the dry season and (ii) a truncated normal distribution (respectively exponential) of mean value λ_{wet} and standard

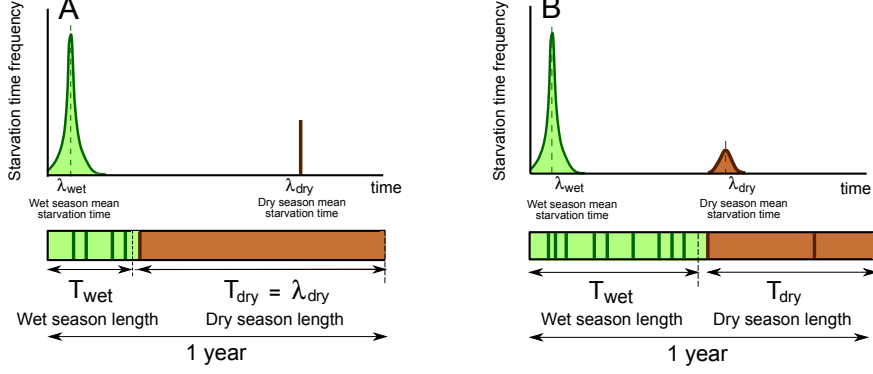


FIG. 3. Implementation of the wet-dry annual seasonality. A) Severe starvation. The year, as represented by the lower bar, is divided into a dry and a wet season whose lengths, T_{wet} and T_{dry} , remain constant over the years. In this scenario, we change the length of the dry season, T_{dry} , to explore its role on the optimal investment in spores. During the dry season, represented by the brown segment, resources do not recover in the limit of $\lambda_{dry} = T_{dry}$. In the wet season however starvation times follow a truncated normal distribution (respectively exponential, not shown) of mean λ_{wet} . For exemplification purposes we show several food pulses; each food pulse is represented by a vertical solid line in the year bar. Dashed black lines represent the values of T_{dry} and T_{wet} . This combination results in a normal distribution for the wet season starvation times and a Dirac delta distribution for the dry season starvation times. B) Milder dry season that allows for nutrient replenishment. In this scenario we fixed the length of both seasons to 6 months in all the simulations. Pulses of resources arrive to the patch but less frequently than during the wet season, $\lambda_{wet} < \lambda_{dry}$. Starvation times follow truncated normal distributions in the dry and the wet season, whose lengths are fixed to 6 months each one.

deviation σ for the wet season.

As a general result the periodic occurrence of long starvation times pushes selection towards higher investment in spores, the higher the longer the dry season is (Fig. 4). This effect is, however, residual if the wet season covers at least 25% of the year (blue squares in Fig. 4). This result follows from the fact that sporadic long starvation times kill all vegetative cells and dramatically decrease the total population of spores, which favors strains with a higher value of α . When spores and non-aggregators constitute a bet-hedging strategy, this result implies that these catastrophic ecological periods promote the evolution of lower-risk strategies, represented by the production of more spores. However, coexistence of bet-hedging strategies is not possible since there is no reproduction during the dry season and thus a second strategy cannot evolve. It is interesting to note that even purely deterministic scenarios in which starvation times during the wet season are constant ($\sigma = 0$), allow the evolution of bet-hedging strategies (Fig. 4A). This results from the alternation in the environmental conditions that reduces the fitness of pure strategies, making

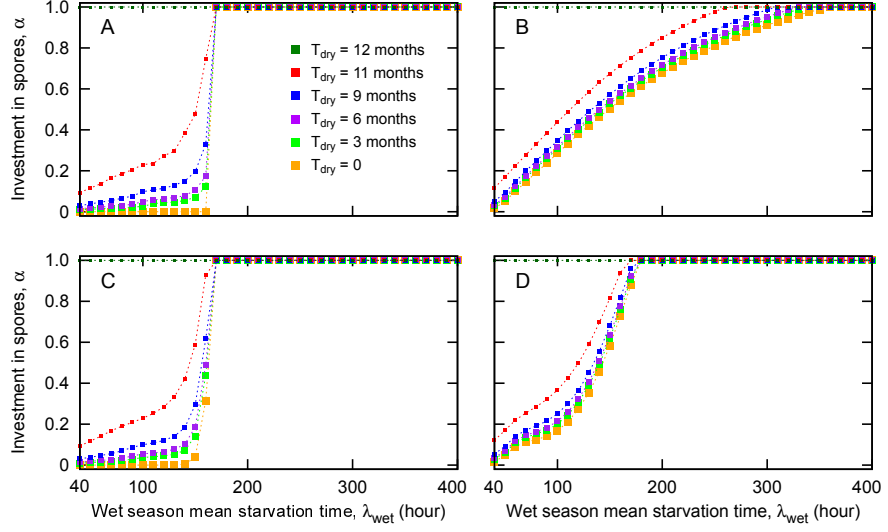


FIG. 4. Effect of a severe dry season ($T_{dry} = \lambda_{dry}$) on the winning genotype. A) Deterministic wet season. B) Exponential environmental variability. C,D) Environmental variability follows a truncated normal distribution, with $\sigma = 20$ (C) and $\sigma = 60$ (D). Simulations are initialized with 1001 genotypes uniformly distributed between $\alpha = 0$ and $\alpha = 1$ and the winner is determined as the most abundant after 2×10^8 hours. A single realization is used in the deterministic case (A) and averages over 20 independent realizations are taken for stochastic scenarios (B, C, D). In all the panels, distinct colors correspond to different lengths of the dry season, from bottom to top: no dry season (orange), 3 months (green), 6 months (purple), 9 months (blue), 11 months (red) and no wet season (dark green).

them suboptimal compared to a mixed investment in aggregators and non-aggregators. Finally, exponentially distributed starvation times have an impact in the winning strategy over a larger set of environments (Fig. 4B), and when starvation times are drawn from a truncated normal, the set of environments dominated by bet-hedging strategies increases with the variance of the distributions, similarly to the case without seasonality (Fig. 4C,D).

2. Milder dry season: slow food recovery

Here we study a less extreme ecological scenario in which pulses of resources also arrive during the dry season, albeit with a lower frequency ($\lambda_{dry} > \lambda_{wet}$). Seasonality is now illustrated by a periodic switching between two distributions with different mean starvation times (Fig. 3B). To simplify the analysis, we fix the length of the seasons and divide the year into 6 months of wet favorable conditions and 6 months of dry harsh environments. To reduce the dimensionality of the parameter space we also fix the mean starvation time in the wet season, $\lambda_{wet} = 50$ hours, and assume

that the intensity of the environmental fluctuations, σ , is the same during both seasons. Although a more realistic approach should account for differences in σ between seasons, this assumption reduces the dimensionality of the parameter space and the complexity of the analysis without qualitatively changing the results presented in this section. The number of parameters reduces thus to two: the mean starvation time in the dry season, λ_{dry} , and the intensity of the fluctuations in both seasons, σ . We find that two strategies, a wet season and a dry season specialist, coexist if two conditions are met (Fig. 5): (i) the starvation times during both seasons are sufficiently different such that there is no overlap between their distributions and two different niches are created within the year (temporal niche partitioning); (ii) each season allows for sufficient growth-starvation cycles for its specialist population to create a storage and survive when it becomes maladapted due to changes in the environment. These two requirements show that coexistence is driven by a temporal storage effect. The third requirement in [11, 24, 30] related to the covariance between interspecific competition and environmental changes, is also implicitly fulfilled: transitions in the seasons penalize the most abundant genotype, whose population starts declining; this reduces interspecific competition and allows the new season specialist to recover from a very low population size. As a result, there is a stable coexistence of two strategies, which oscillate with a period that depends on the length of the seasons (Fig. 5D) [19].

Temporal niche partitioning requires an upper bound in the intensity of the fluctuations. Environments with high variability result in wider distributions for the starvation times, which increases the overlap between the distributions of wet and dry season starvation times. This tends to eliminate the temporal niche partitioning and, as a consequence, coexistence is lost. Similarly, for a fixed level of environmental variability (i.e. width of the distributions of starvation times) more similar mean values also tend to increase the overlap between the distributions of seasonal starvation times and the range of reduce coexistence. Since we keep the mean starvation time of the wet season constant, this latter condition introduces a lower limit for the mean starvation time of the dry season in order for coexistence to be maintained. In addition, the requirement for several growth-starvation cycles excludes extremely high mean starvation times from the region of coexistence in the parameter space (Fig. 5A).

Finally, we study how surviving strategies vary as the ecological variables (i.e. dry season mean starvation time and amplitude of the environmental variability) change. Due to the fixed length of the seasons, the number of growth-starvation cycles that they permit decreases as the mean starvation time increases. This implies a reduction in the number of generations and therefore in the evolutionary impact of a season on the winning strategy. For the case studied in Figure 5

(Fig. 5B, dashed-line transect of Fig. 5A), in which the length of both seasons is fixed to 6 months and the mean starvation time in the wet season is fixed to 50 hours, the number of generations within the dry season decreases as λ_{dry} increases. Consequently, selection favors strategies with a lower investment in spores and coexistence is eventually lost in the limit of high λ_{dry} , in which very few reproduction events take place during the dry season. This result should not be confused with the scenario tackled in Section III B 1, in which higher values of λ_{dry} lead to investment in more spores. In that case, season length is determined by λ_{dry} , with higher values of λ_{dry} leading to larger dry seasons and shorter wet periods.

As far as the environmental variability is concerned, medium to higher values of σ force the loss of one of the strains (Fig. 5C, dashed-line transect of Fig. 5A). In this case the temporal niche partitioning is lost due to the increased overlap between the wet and dry distributions, which increases the similarity of starvation times between seasons. Consequently, one of the evolving strategies has a sufficiently high fitness in all the periods of the year to outcompete specialist strategies. The winner always evolves from the former wet season specialist because most of the growth-starvation cycles occur in that part of the year, increasing the annual fitness of strains with a low investment in spores and amplifying the storage effect of the wet season winner over the dry season one.

Finally, if starvation times are drawn from exponential distributions there is no coexistence because the two distributions always have a large overlap. In this case, despite having different mean values in each season, most starvation periods are short throughout the year and an annual generalist bet-hedging strategy evolves.

C. Diversity promoted by additional life-history tradeoffs

Finally, we consider the full model, in which the division rate c (assumed to be inversely proportional to cell size) is an evolving trait that contributes to the fitness of each genotype and leads to two additional tradeoffs [4]: one between spore viability and division rate and another between starving cell survival and division rate. Smaller cells (higher division rates) are less resistant to starvation and produce spores with a lower viability (Fig. 1B). In this complete framework a third strategy, an annual bet-hedger, can coexist with the two season specialist bet-hedging strategies. This occurs when the dry season has a low mean starvation time and both seasons have low variability (Fig. 6A-E), since the existence of an annual bet-hedger requires seasons to be sufficiently similar and have a low level of environmental variability. At higher environmental variabilities the

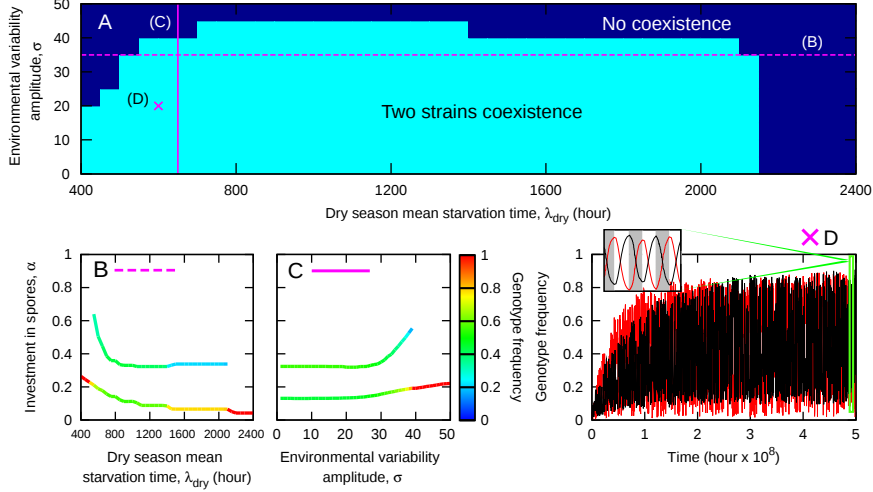


FIG. 5. Coexistence of two strains is possible when the dry season allows resource replenishment, albeit more slowly than the wet one. Parameters: $T_{wet} = 6$ months, $T_{dry} = 6$ months, $\lambda_{wet} = 50$ hours. A) Regions of coexistence in the parameter space defined by the amplitude of the environmental variability (taken to be equal in both seasons) and the mean starvation time in the dry season. The space is scanned with a resolution given by $\Delta\sigma = 5$ and $\Delta\lambda_{dry} = 50$. Simulations are started with 1001 genotypes and coexistence evaluated by the number of surviving species after 2×10^8 hours, averaged over 20 independent realizations. The dashed (solid) magenta line and the magenta cross indicate the region of the parameter space used in panels B (C) and D respectively. B) Surviving genotypes as a function of the dry season mean starvation time for a fixed environmental variability amplitude, $\sigma = 35$. The color of the line changes according to the frequency of each genotype. The frequency is obtained by taking averages at the end of each season from $t = 1.5 \times 10^8$ to $t = 2 \times 10^8$ hours. C) Same as B but keeping $\lambda_{dry} = 650$ hours constant and varying σ . D) Time series of the two coexisting genotypes, $\alpha = 0.142$ (red) and $\alpha = 0.324$ (black). The inset shows a zoom on the interval marked by the green window, gray time intervals correspond to the wet season and white intervals to the dry season.

differences between seasons are blurred by the effect of the fluctuations; then, the specialists are able to survive at higher population sizes during adverse periods and they outcompete any annual bet-hedgers. Eventually, as we already showed in Section III B 2, as the intensity of environmental fluctuations keeps increasing, the temporal niche partitioning is lost (the overlap between distributions in Fig. 3B increases) and a single strategy emerges that dominates all ecological scenarios.

In this full model in which the division rate changes across genotypes, the length of the growing phase, in addition to the number of growth-starvation cycles, plays an important role. It determines the payoff resulting from a higher division rate (i.e. the production of more but smaller progeny) and whether this is sufficient to overcome the cost of those progeny becoming less viable spores

and less likely to survive vegetative cells. The time between the arrival of the food pulse and its complete depletion is determined by the total population size and its genotypic composition, which defines the strength of the competition for resources. At low population sizes the competition for resources is lower and the growth periods larger. This favors higher reproduction rates since they result in more offspring that compensate for the higher cost of reduced cell/spore size. However, as the total population size increases, the growth phases become shorter. Then, strains with a higher division rate do not have time to create a sufficiently large number of progeny; in that case, selection favors genotypes that reproduce more slowly but make larger cells/spores, which have an increased survival/viability. Following this rationale, we can explain the behavior of the optimal division rate in Figures 6C and 6E. At the end of the wet season the total population size is large, so the annual bet-hedger, which has the smaller reproduction rate, is favored. Then, as the wet-seasons specialist declines, the feeding periods become longer and the dry season specialist, with a higher reproduction rate, starts outcompeting the annual bet-hedger. Due to the transient dynamics in each season, annual bet-hedgers show oscillations with a frequency that is approximately twice the frequency of the oscillation in the season-specialist populations (inset of Fig. 6F). Finally, the optimal investment in spores (Fig. 6B and 6D) behaves as in the simpler case where division rate is fixed, and it can be explained using the same arguments introduced in Section III B 2.

IV. CONCLUSIONS

We investigate theoretically the scenarios under which temporal heterogeneity, here captured through the existence of a wet and dry season, drives the coexistence of competing bet-hedging strategies in microbial populations. We further explore the interplay between coexistence and the number of life history traits and tradeoffs. Our main focus is on the cellular slime mold *D. discoideum*, which has recently been proposed as an example of bet-hedging in microbes [5, 6, 37] and which shows a vast genetic diversity in nature [3]. However, the model can be easily extended to other microbes and the results are likely general.

The evolution of bet-hedging strategies is driven by environmental stochasticity for various sources of fluctuations, such as exponential [6], uniform [5] and, as studied here, truncated normal distributions. For the latter the effect of the mean value and the amplitude of the fluctuations can be studied separately and we showed that more intense fluctuations select for strategies with a higher investment in spores. However, we pose the more general question: what is the minimal set of conditions under which a single strategy is not able to average (hedge its bets) over the

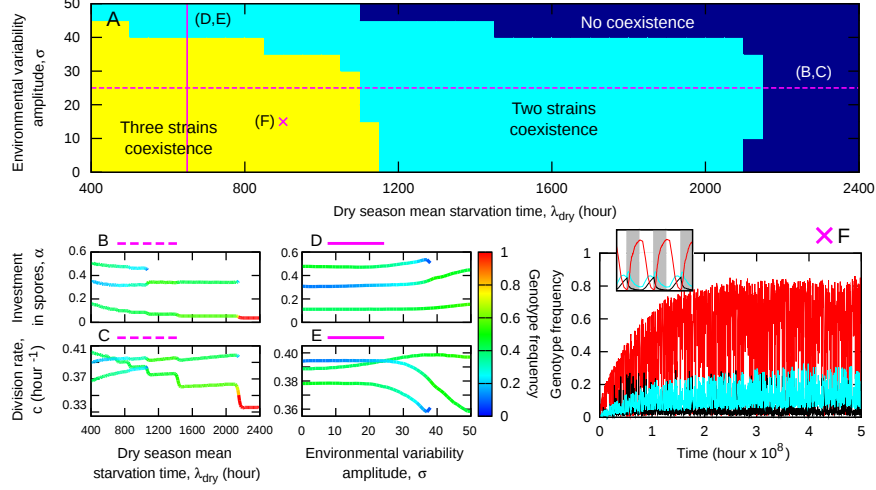


FIG. 6. Strain diversity increases when multiple tradeoffs are included. Parameters: $T_{wet} = 6$ months, $T_{dry} = 6$ months, $\lambda_{wet} = 50$ hours. A) Regions of coexistence in the parameter space defined by the amplitude of the environmental variability (taken to be the same in both seasons) and the mean starvation time in the dry season. The space is scanned with a resolution given by $\Delta\sigma = 5$ and $\Delta\lambda_{dry} = 50$. Simulations are started with 401401 genotypes (1001 values of α between 0 and 1 and 401 values of c between 0.05 and 0.45) and coexistence evaluated by the number of surviving species after 2×10^8 hours, averaged over 20 independent realizations. The dashed (solid) magenta line and the magenta cross indicate the region of the parameter space used in panels B, C (D, E) and F respectively. B,C) Surviving genotypes defined by α (B) and c (C) as a function of the dry season mean starvation time for a fixed environmental variability amplitude, $\sigma = 25$. The color of the line changes according to the frequency of each genotype. The frequency is calculated by taking averages at the end of each season from $t = 1.5 \times 10^8$ to $t = 2 \times 10^8$ hours. D, E) Same as B and C but keeping $\lambda_{dry} = 650$ hours constant and varying σ . F) Time series of the three coexisting genotypes: $\alpha = 0.085$, $c = 0.380$ (red); $\alpha = 0.324$, $c = 0.390$ (black) and $\alpha = 0.488$, $c = 0.380$ (cyan). The inset shows a zoom on the interval marked by the green window, gray time intervals correspond to the wet season and white intervals to the dry season.

different environmental contexts and is replaced, via temporal niche partitioning and a temporal storage effect, by coexisting season specialists? We investigate two different patterns of seasonality determined by the behavior of the dry season. First we studied a severe dry season, represented by a single starvation period that spans the entire season. In this scenario, since reproduction only takes place in the presence of food, wet seasons permit many more generations than dry seasons, which only act as catastrophic perturbations that favor selection for higher investment in spores (lower-risk strategies). This result is consistent with previous studies in annual plants that showed how catastrophic years favor the evolution of lower risk germination strategies [25]. Second, we studied a milder dry season that allows for growth cycles, albeit fewer than the wet

one. We showed that this can drive the evolution of season-specialist bet-hedging strategies that stably coexist via a temporal storage effect [11, 24, 30]. Two conditions have to be fulfilled: (i) no overlapping between the seasonal distributions of starvation times to ensure temporal niche partitioning and (ii) numerous growth-starvation cycles occurring within each season to create a storage of each strain and guarantee its survival under adverse conditions. The constraints in the overlap between the distributions of starvation times imposed by the first condition, do not allow to get coexistence driven by exponentially distributed starvation times.

Finally, an extended model that considers additional genotypic traits under selection and multiple tradeoffs mediated by these traits makes possible the coexistence of more than two strains. This is consistent with existing results that emphasize the importance of tradeoffs in establishing species coexistence [11, 32, 35, 43, 44]. The additional trait we consider for *D. discoideum* is the division rate, which yields tradeoffs between cell size and spore viability and vegetative cell resistance to starvation [4]. In addition to the dry and the wet season specialists, a third annual bet-hedging strain is able to persist by growing at the beginning of each season, when interspecific competition is low and under conditions that prevent either of the specialists from completely outcompeting it by the end of the season. This is consistent with previous studies in annual plants, where a tradeoff between seed survivorship and seed yield was shown to increase the set of environments where coexistence is possible [25]. However, we extend these existing results and show that not only the number of environments can increase, but also the number of coexisting species.

Our results highlight the importance of ecological variables along with multiple fitness components and tradeoffs among them in explaining long-term strain coexistence in *D. discoideum*. However, the well-mixed approach we used here neglects the effect of spatial degrees of freedom that may also play an important role [6, 12, 45–48]. Exploring whether a combination of temporal and spatial heterogeneity expands the set of ecological scenarios in which coexistence may be found as well as the number of coexisting species arises as a natural extension of this work. Our framework also omits the existence of cell-to-cell interactions that occur during aggregation and fruiting body development; including these could modify the investment in spores in mixed populations as compared to clonal scenarios [49] and should be investigated in future work. In addition, diversity in the dietary preferences also needs to be studied further as a potential promoter of coexistence [50]. Finally, diversifying the sources of ecological uncertainty between the starving (mean starvation times) and the growing phase (amount and quality of the resources) would provide a more complete picture of the ecological forces that drive the coexistence of bet-hedging strategies.

ACKNOWLEDGMENTS

We thank the IFISC (CSIC-UIB) computing lab for technical support and the use of their computational resources and the Alfred P. Sloan Foundation for funding. We are grateful to Joan E. Strassmann for suggesting the study of seasonality in *D. discoideum* and to George W.A. Constable for useful discussions.

Appendix A: Generation of truncated normal distributions

A truncated normal distribution is usually defined in two steps: (i) choosing a standard normal distribution, called parent distribution, of parameters $(\bar{\mu}, \bar{\sigma})$ and (ii) specifying a truncation range (a, b) . The probability density function (PDF) of the truncated distribution is obtained by setting the values of the original PDF to zero outside the truncation range and uniformly rescaling the values inside the range so that the norm is 1. The truncation changes the mean value and the standard deviation of the original normal distribution. These new values correspond in the model with the mean starvation time, λ_T , and the environmental variability amplitude, σ , respectively.

The truncated distribution will be symbolized by $\psi(\bar{\mu}, \bar{\sigma}, a, b; t)$ and its parental standard normal distribution by $N(\bar{\mu}, \bar{\sigma}; t)$. We will work with $a = 0$, $b = \infty$ and t will be the length of the starvation period. To obtain which distribution has the desired mean value λ_T and standard deviation σ one has to obtain the parental distribution solving:

$$\int_0^\infty \psi(\bar{\mu}, \bar{\sigma}, a, b; t) dt = \int_0^\infty K N(\bar{\mu}, \bar{\sigma}; t) dt = 1, \quad (A1)$$

$$\int_0^\infty \psi(\bar{\mu}, \bar{\sigma}, a, b; t) t dt = \int_0^\infty K N(\bar{\mu}, \bar{\sigma}; t) t dt = \lambda_T, \quad (A2)$$

$$\int_0^\infty \psi(\bar{\mu}, \bar{\sigma}, a, b; t) t^2 dt - \lambda_T^2 = \int_0^\infty K N(\bar{\mu}, \bar{\sigma}; t) t^2 dt - \lambda_T^2 = \sigma^2, \quad (A3)$$

that gives the following system of equations that can be solved for each pair of (λ_T, σ) values

$$\frac{1}{2} K \left[1 + \text{Err} \left(\frac{\bar{\mu}}{\sqrt{2}\bar{\sigma}} \right) \right] = 1 \quad (A4)$$

$$\frac{1}{2} K \left[\bar{\mu} + \sqrt{\frac{2}{\pi}} \bar{\sigma} \exp \left(-\frac{\bar{\mu}^2}{2\bar{\sigma}^2} \right) + \bar{\mu} \text{Err} \left(\frac{\bar{\mu}}{\sqrt{2}\bar{\sigma}} \right) \right] = \lambda_T \quad (A5)$$

$$\frac{\bar{\mu} \bar{\sigma}}{\sqrt{2\pi}} K \exp \left(-\frac{\bar{\mu}^2}{2\bar{\sigma}^2} \right) + \frac{1}{2} K (\bar{\mu}^2 + \bar{\sigma}^2) \left[1 + \text{Err} \left(\frac{\bar{\mu}}{\sqrt{2}\bar{\sigma}} \right) \right] - \lambda_T^2 = \sigma^2 \quad (A6)$$

where $\text{Err}(x) = \sqrt{\frac{2}{\pi}} \int_0^x e^{-t^2} dt$ is the error function. To solve numerically Eqs. (A5) and (A6) we

use an approximation to the error function given by [51]

$$\text{Err}(x) = \begin{cases} -1 + \sum_{i=1}^5 a_i f(x)^i e^{-x^2} & \text{if } x \leq 0 \\ 1 - \sum_{i=1}^5 a_i f(x)^i e^{-x^2} & \text{if } x > 0 \end{cases} \quad (\text{A7})$$

where $f(x) = \frac{1}{(1+p|x|)}$ with $p = 0.32759$. The values of the coefficients are $a_1 = 0.254829$, $a_2 = -0.284496$, $a_3 = 1.421413$, $a_4 = -1.453152$, $a_5 = 1.061405$.

Appendix B: Simulation of the truncated normal distribution

We use two methods to simulate the truncated distribution:

1. If $\bar{\mu} \geq 0$ we sort random numbers following the parental normal distribution. They are rejected whenever they are negative and a new number is sorted until getting a positive value.
2. If $\bar{\mu} < 0$ the previous method may be extremely inefficient as the number of rejections increases with decreasing $\bar{\mu}$. In this case we use an acceptance-rejection method [52]. The basic idea is to find an alternative probability distribution G such that we already have an efficient algorithm for generating random numbers and that its density function $g(t)$ is similar to the truncated normal distribution, $\psi(\bar{\mu}, \bar{\sigma}, a, b; t)$. The steps of the algorithm are:
 - (a) Generate a random number U_1 distributed as G .
 - (b) Generate a random number U_2 from a uniform distribution in the interval $[0, 1]$.
 - (c) If:

$$U_2 \leq \frac{\psi(U_1)}{g(U_2)} \quad (\text{B1})$$

then accept U_1 ; otherwise go back to 1 and generate a new number.

Therefore, in order to minimize the number of rejections, the ratio $\psi(\bar{\mu}, \bar{\sigma}, a, b; t)/g(t)$ has to be lower but as close as possible to 1 for all t . We work with $g(t) = 1.3N(\bar{\mu}, \bar{\sigma}; 0) \exp(-0.01t)$ which approximates the tail of the parental normal distributions $N(\bar{\mu}, \bar{\sigma}; t)$ when $\bar{\mu} \ll 0$ and gives a high percentage of acceptances.

[1] J. T. Bonner, *The social amoebae: the biology of cellular slime molds*. Princeton University Press, 2009.

- [2] A. Fortunato, D. C. Queller, and J. E. Strassmann, “A linear dominance hierarchy among clones in chimeras of the social amoeba *Dictyostelium discoideum*,” *Journal of evolutionary biology*, vol. 16, pp. 438–45, may 2003.
- [3] A. Fortunato, J. E. Strassmann, L. Santorelli, and D. C. Queller, “Co-occurrence in nature of different clones of the social amoeba, *Dictyostelium discoideum*,” *Molecular ecology*, vol. 12, pp. 1031–8, apr 2003.
- [4] J. B. B. Wolf, J. A. A. Howie, K. Parkinson, N. Gruenheit, D. Melo, D. Rozen, and C. R. Thompson, “Fitness trade-off result in the illusion of social success,” *Current Biology*, vol. 25, no. 8, pp. 1086–1090, 2015.
- [5] D. Dubravcic, M. van Baalen, and C. Nizak, “An evolutionarily significant unicellular strategy in response to starvation stress in *Dictyostelium* social amoebae,” *F1000Research*, vol. 3, no. 133, pp. 1–24, 2014.
- [6] C. E. Tarnita, A. Washburne, R. Martinez-Garcia, A. E. Sgro, and S. a. Levin, “Fitness tradeoffs between spores and nonaggregating cells can explain the coexistence of diverse genotypes in cellular slime molds,” *Proceedings of the National Academy of Sciences*, vol. 112, pp. 2776–2781, mar 2015.
- [7] R. Martinez-Garcia and C. E. Tarnita, “Lack of Ecological Context Can Create the Illusion of Social Success in *Dictyostelium discoideum*,” *arXiv preprint*, 2016.
- [8] D. Tilman, *Resource Competition and Community Structure*. Princeton University Press, 1982.
- [9] G. Hardin, “The competitive exclusion principle,” 1960.
- [10] R. D. Holt, J. Grover, and D. Tilman, “Simple Rules for Interspecific Dominance in Systems with Exploitative and Apparent Competition,” *The American Naturalist*, vol. 144, no. 5, pp. 741–771, 1994.
- [11] P. Chesson, “Mechanisms of Maintenance of Species Diversity,” *Annual Review of Ecology and Systematics*, vol. 31, no. 1, pp. 343–366, 2000.
- [12] P. Amarasekare, “Competitive coexistence in spatially structured environments: A synthesis,” *Ecology Letters*, vol. 6, no. 12, pp. 1109–1122, 2003.
- [13] D. Gravel, F. Guichard, and M. E. Hochberg, “Species coexistence in a variable world,” *Ecology Letters*, vol. 14, no. 8, pp. 828–839, 2011.
- [14] J. M. Chase and M. A. Leibold, *Ecological Niches: Linking Classical and Contemporary Approaches*. University of Chicago Press, 2003.
- [15] T. Philippi and J. Seger, “Hedging One’s Evolutionary Bets, Revisited,” *Trends in Ecology & Evolution*, vol. 4, no. 2, pp. 2–5, 1989.
- [16] I. G. De Jong, P. Haccou, and O. P. Kuipers, “Bet hedging or not? A guide to proper classification of microbial survival strategies,” *BioEssays*, vol. 33, no. 3, pp. 215–223, 2011.
- [17] J. Seger and H. J. Brockmann, “What is bet-hedging?,” in *Oxford Surveys in Evolutionary Biology. Volume 4*, pp. 182–211, Oxford, 1987.
- [18] A. M. Simons, “Modes of response to environmental change and the elusive empirical evidence for bet hedging,” *Proceedings of the Royal Society B: Biological Sciences*, vol. 278, no. 1712, pp. 1601–1609,

2011.

[19] J. Ripa, H. Olofsson, and N. Jonzén, “What is bet-hedging, really?,” *Proceedings of the Royal Society B*, vol. 277, pp. 1153–1154, 2010.

[20] P. Chesson, “Multispecies competition in variable environments,” *Theoretical Population Biology*, vol. 45, pp. 227–276, 1994.

[21] P. Chesson and N. Huntly, “Temporal hierarchies of variation and the maintenance of diversity,” 1993.

[22] P. B. Adler, J. HilleRisLambers, P. C. Kyriakidis, Q. Guan, and J. M. Levine, “Climate variability has a stabilizing effect on the coexistence of prairie grasses.,” *Proceedings of the National Academy of Sciences of the United States of America*, vol. 103, no. 34, pp. 12793–12798, 2006.

[23] D. Tilman and S. W. Pacala, “The maintenance of species richness in plant communities,” in *Species Diversity in Ecological Communities* (R. Ricklefs and D. Schlüter, eds.), pp. 13–25, University of Chicago Press, 1993.

[24] P. Chesson and R. R. Warner, “Environmental variability promotes coexistence in lottery competitive systems,” *The American Naturalist*, vol. 117, no. 6, pp. 923–943, 1981.

[25] S. Ellner, “Alternate plant life history strategies and coexistence in randomly varying environments,” *Vegetation*, vol. 69, no. 1-3, pp. 199–208, 1987.

[26] J. M. Facelli, P. Chesson, and N. Barnes, “Differences in seed biology of annual plants in arid lands: A key ingredient of the storage effect,” *Ecology*, vol. 86, no. 11, pp. 2998–3006, 2005.

[27] D. Cohen, “Optimizing reproduction in a randomly varying environment.,” *Journal of theoretical biology*, vol. 12, no. 1, pp. 119–129, 1966.

[28] D. Z. Childs, C. J. E. Metcalf, and M. Rees, “Evolutionary bet-hedging in the real world: empirical evidence and challenges revealed by plants.,” *Proceedings of the Royal Society B*, vol. 277, no. 1697, pp. 3055–3064, 2010.

[29] D. L. Venable, “Bet hedging in a guild of desert annuals,” *Ecology*, vol. 88, no. 5, pp. 1086–1090, 2007.

[30] P. L. Chesson, “Coexistence of competitors in a stochastic environment: the storage effect,” in *Proceedings of the International Conference held at the University of Alberta, Edmonton, Canada, June 2230, 1982* (H. I. Freedman and C. Strobeck, eds.), pp. 188–198, Springer Berlin Heidelberg, 1983.

[31] S. Venner, P.-F. Pélisson, M.-C. Bel-Venner, F. Débias, E. Rajon, and F. Menu, “Coexistence of Insect Species Competing for a Pulsed Resource: Toward a Unified Theory of Biodiversity in Fluctuating Environments,” *PLoS ONE*, vol. 6, no. 3, p. e18039, 2011.

[32] A. L. Angert, T. E. Huxman, P. Chesson, and D. L. Venable, “Functional tradeoffs determine species coexistence via the storage effect.,” *Proceedings of the National Academy of Sciences of the United States of America*, vol. 106, no. 28, pp. 11641–11645, 2009.

[33] P. Chesson, R. L. E. Gebauer, S. Schwinning, N. Huntly, K. Wiegand, M. S. K. Ernest, A. Sher, A. Novoplansky, and J. F. Weltzin, “Resource pulses, species interactions, and diversity maintenance in arid and semi-arid environments,” *Oecologia*, vol. 141, no. 2, pp. 236–253, 2004.

- [34] R. Kassen and P. B. Rainey, "The Ecology and Genetics of Microbial Diversity," *Annual Review of Microbiology*, vol. 58, no. 1, pp. 207–231, 2004.
- [35] B. J. M. Bohannan, B. Kerr, C. M. Jessup, J. B. Hughes, and G. Sandvik, "Trade-offs and coexistence in microbial microcosms," *Antonie van Leeuwenhoek, International Journal of General and Molecular Microbiology*, vol. 81, no. 1-4, pp. 107–115, 2002.
- [36] N. R. Pace, "A Molecular View of Microbial Diversity and the Biosphere," *Science*, vol. 276, pp. 734–740, may 1997.
- [37] A. J. Grimbergen, J. Siebring, A. Solopova, and O. P. Kuipers, "Microbial bet-hedging: the power of being different," *Current Opinion in Microbiology*, vol. 25, pp. 67–72, 2015.
- [38] W. C. Ratcliff and R. F. Denison, "Individual-level bet hedging in the bacterium *Sinorhizobium meliloti*," *Current Biology*, vol. 20, no. 19, pp. 1740–1744, 2010.
- [39] a. Solopova, J. van Gestel, F. J. Weissing, H. Bachmann, B. Teusink, J. Kok, and O. P. Kuipers, "Bet-hedging during bacterial diauxic shift," *Proceedings of the National Academy of Sciences*, vol. 111, no. 20, pp. 7427–7432, 2014.
- [40] D. Dubravcic, *Quantitative evolutionary analysis of the life cycle of social amoebae PhD committee* : PhD thesis, Universite Rene Descartes - Paris V, 2013.
- [41] J. Monod, "The growth of bacterial cultures," *Annual Review of Microbiology*, vol. 3, pp. 371–394, 1949.
- [42] G. P. Otto, M. Y. Wu, N. Kazgan, O. R. Anderson, and R. H. Kessin, "Dictyostelium Macroautophagy Mutants Vary in the Severity of Their Developmental Defects," *Journal of Biological Chemistry*, vol. 279, no. 15, pp. 15621–15629, 2004.
- [43] D. Tilman, "Constraints and Tradeoffs: Toward a Predictive Theory of Competition and Succession," *Oikos*, vol. 58, no. 1, pp. 3–15, 1990.
- [44] T. L. S. Vincent, D. Scheel, J. S. Brown, and T. L. Vincent, "Trade-Offs and Coexistence in Consumer-Resource Models : It all Depends on what and where you Eat," vol. 148, no. 6, pp. 1038–1058, 1996.
- [45] P. Chesson, "General theory of competitive coexistence in spatially-varying environments.," *Theoretical Population Biology*, vol. 58, no. 3, pp. 211–37, 2000.
- [46] A. Buckling, R. Kassen, G. Bell, and P. B. Rainey, "Disturbance and diversity in experimental microcosms.," *Nature*, vol. 408, no. 6815, pp. 961–964, 2000.
- [47] R. D. Holt, "Spatial Heterogeneity , Indirect Interactions , and the Coexistence of Prey Species," *The American Naturalist*, vol. 124, no. 3, pp. 377–406, 1984.
- [48] R. E. Snyder and P. Chesson, "Local dispersal can facilitate coexistence in the presence of permanent spatial heterogeneity," *Ecology Letters*, vol. 6, no. 4, pp. 301–309, 2003.
- [49] K. Uchinomiya and Y. Iwasa, "Evolution of stalk/spore ratio in a social amoeba: Cell-to-cell interaction via a signaling chemical shaped by cheating risk," *Journal of Theoretical Biology*, vol. 336, pp. 110–118, 2013.

- [50] E. G. Horn, “Food Competition Among the Cellular Slime Molds (Acrasieae),” *Ecology*, vol. 52, no. 3, pp. 475–484, 1971.
- [51] M. Abramowitz and I. A. Stegun, *Handbook of mathematical functions: with formulas, graphs, and mathematical tables*. No. 55, Courier Corporation, 1964.
- [52] J. E. Gentle, *Random number generation and Monte Carlo methods*. Springer Science & Business Media, 2006.